JACS
JOURNAL OF THE AMERICAN CHEMICAL SOCIETY
Article
pubs.acs.org/JACS

Allosteric Regulation of Unidirectional Spring-like Motion of Double-Stranded Helicates

Yoshimasa Suzuki, Taiki Nakamura, Hiroki Iida,† Naoki Ousaka, and Eiji Yashima*

Department of Molecular Design and Engineering, Graduate School of Engineering, Nagoya University, Chikusa-ku, Nagoya 464-8603, Japan

Supporting Information

ABSTRACT: We report the unprecedented allosteric regulation of the extension and contraction motions of double-stranded spiroborate helicates composed of 4,4′-linked 2,2′-bipyridine (bpy) and its *N*,*N*′-dioxide units in the middle of *ortho*-linked tetraphenol strands. NMR and circular dichroism measurements and an X-ray crystallographic analysis along with theoretical calculations revealed that enantiomeric helicates contract and extend upon the binding and release of protons and/or metal ions at the covalently linked two binding bpy or *N*,*N*′-dioxide moieties without racemization, respectively, regulated by a cooperative *anti*−*syn* conformational change of the two bpy or *N*,*N*′-dioxide moieties. These *anti*−*syn* conformational changes that occurred at the linkages are amplified into a large-scale molecular motion of the helicates leading to reversible spring-like motions coupled with twisting in one direction in a highly homotropic allosteric fashion.

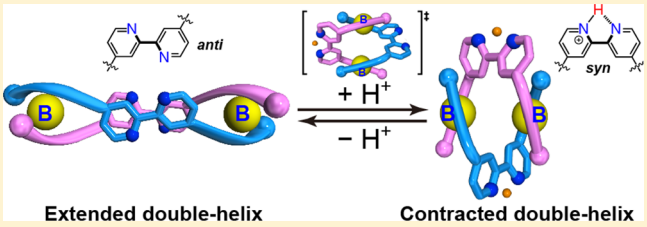

INTRODUCTION

Positive cooperative binding of substrates or ions to different binding sites within biological polymers is ubiquitous in living systems as is observed in allosteric proteins and enzymes, where the binding of a first substrate or ion facilitates the following binding events as a result of specific conformational transitions of the allosteric receptors.[1] The application of such a positive allostery to control functions, such as host−guest molecular recognition, signal amplification, and catalysis has rapidly evolved into one of the intriguing research areas in supramolecular chemistry.[2] Since the host−guest binding can induce a conformational change in artificial allosteric receptors,[2] the molecular design concepts of allosteric systems are relevant to those of molecular machines[3] responsible for external stimuli, which, however, usually trigger a smaller amplitude of molecular motion. Hence, the development of synthetic allosteric receptors that exhibit a sufficiently large-amplitude conformational change, such as a muscle-like extension−contraction molecular motion, still remains a challenge.[3a,c,d,g,l,m] Among the artificial systems showing such elastic motions,[3a,c,d,g,l,m] helical molecules, in particular, have a distinct advantage over other structural motifs due to their inherently chiral structures that enable a fascinating unidirectional twisting motion during the extension−contraction process. Although several synthetic helical oligomers and polymers display such extension−contraction motions in response to external stimuli,[4] these helices have rarely undergone a unidirectional spring-like motion.

We previously reported a unique optically active double-stranded helicate **1a** composed of two spiroborate moieties doubly bridged by two *ortho*-linked tetraphenol ligands with a biphenylene linker in the middle in which a Na^+ ion is embedded in the center of the helicate coordinated by the oxygen atoms of the spiroborate moieties (Figure 1a).[5] This helicate underwent a Na^+ ion-triggered unidirectional spring-like motion upon the release and binding of the Na^+ ion (Figure 1b).[6] However, when *ortho*-linked biphenol[7] (**1b**) and 6,6′-linked 2,2′-bipyridine[8] (bpy) linkers (**2**) were used instead of the biphenylene linker (Figure 1a), the Na^+ ions could not be removed from the center of the contracted helicates **1b** and **2** even by using [2.2.1]-cryptand as a strong receptor for the Na^+ ion, which was able to extract the Na^+ ion from **1a**, thus leading to no extension−contraction motions.[7,8] This is due to the strong coordination of the central Na^+ ions to the biphenol oxygen and bpy nitrogen atoms of the linker units, in which these heteroatoms are directed toward the inside of the central cavity.

In order to further develop an intelligent molecular spring responsible for the complexation with various guest molecules as well as the Na^+ ion,[9] we have designed and synthesized novel double-stranded spiroborate helicates, $\mathbf{DH3}_{\mathbf{TBA2}}$ and $\mathbf{DH4}_{\mathbf{TBA2}}$ (TBA = tetrabutylammonium), composed of two tetraphenol strands bearing 4,4′-linked 2,2′-bpy and its bpy *N*,*N*′-dioxide units in the middle, respectively,[10] instead of the 6,6′-linked bpy units, in which the nitrogen atoms are likely located toward the outside of the helicates in their contracted forms (Figure 1c). Therefore, we anticipated that the helicates would exhibit a similar unidirectional spring-like motion triggered by the binding and release of protons and/or metal ions that will occur at the two covalently linked binding bpy or *N*,*N*′-dioxide moieties with the accompanying *anti*-*syn* conformational change,[11] thereby

Received: January 22, 2016
Published: February 24, 2016

DOI: 10.1021/jacs.6b00787
J. Am. Chem. Soc. 2016, 138, 4852−4859

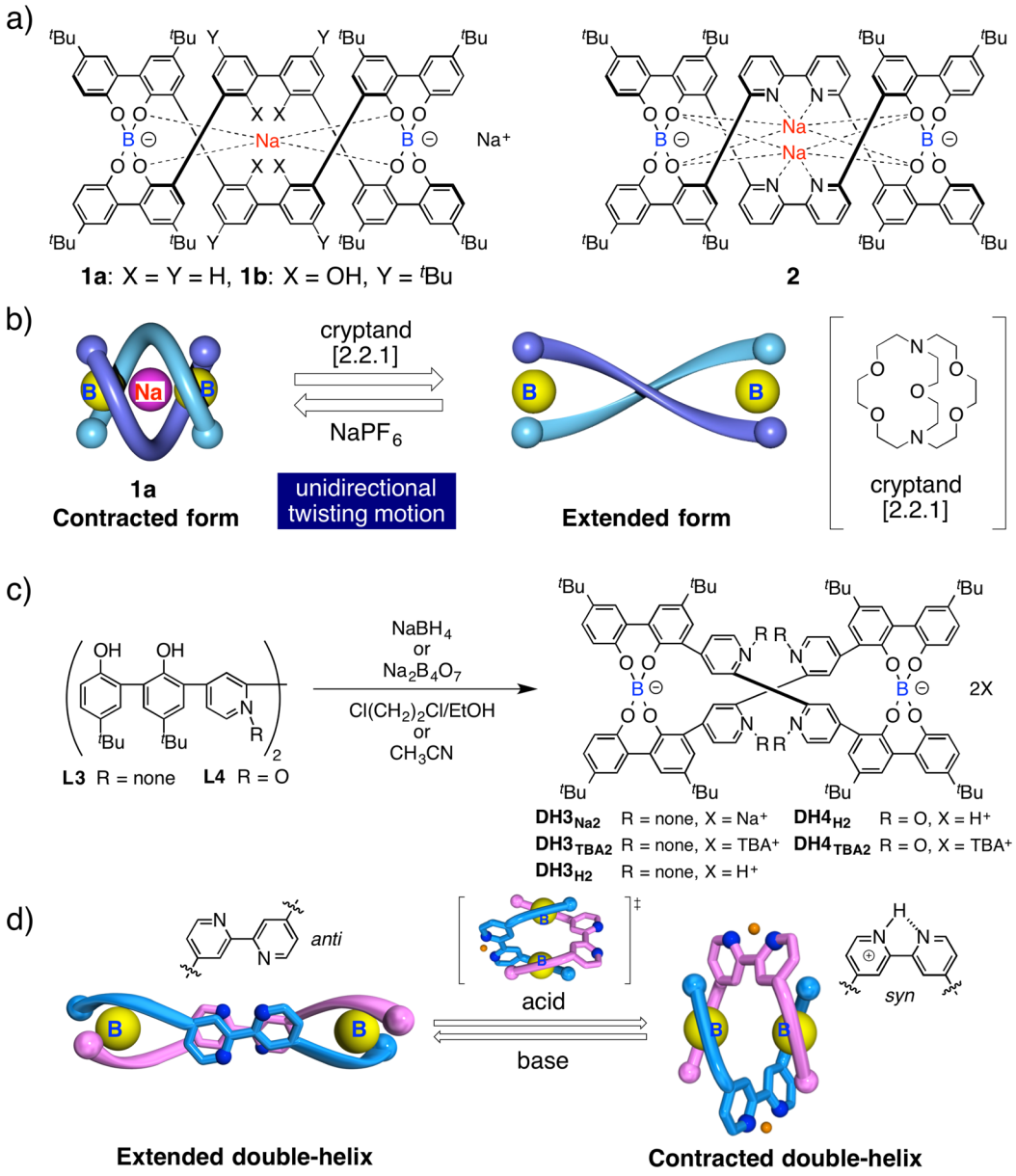

Figure 1. (a) Chemical structures of double-stranded spiroborate helicates **1a**, **1b**, and **2**. (b) Schematic representation of the unidirectional spring-like motion upon Na^+-ion release and binding. (c) Synthesis of double-stranded spiroborate helicates $\mathbf{DH3}_{X2}$ and $\mathbf{DH4}_{X2}$ (X = Na^+, TBA^+, or H^+). (d) Schematic representation of acid/base-triggered reversible extension–contraction motion of $\mathbf{DH3}^{2-}$ through the positive cooperative H^+ binding that induces *anti*-to-*syn* isomerization of the 2,2′-bipyridine units of $\mathbf{DH3}^{2-}$.

enabling the unidirectional twisting motion in a highly cooperative, allosteric manner (Figure 1d). To the best of our knowledge, artificial molecular machines showing reversible extension–contraction motions triggered by the multiple binding of substrates (or protons) in a positive allosteric fashion have never been achieved, despite such dynamic molecular motions coupled with a positive allosterism being highly relevant to and required for biological machinery systems.[12]

RESULTS AND DISCUSSION

The double-stranded helicates ($\mathbf{DH3}_{Na2}$ and $\mathbf{DH4}_{H2}$[13]) bearing the bpy and its *N*,*N*′-dioxide linkages were prepared according to Scheme S1 (Supporting Information) by the reactions of the corresponding ligands **L3** and **L4** with $NaBH_4$ (1 equiv) in 1,2-dichloroethane/EtOH (6/1, v/v) at 80 °C and with $Na_2B_4O_7$ (1 equiv) in CH_3CN at 70 °C under conditions similar to those used for the synthesis of the related spiroborate helicates in good yields (80 and 90%), respectively (Figure 1c).[5,7,8,14] Counter-cation exchange with protons using trifluoroacetic acid (TFA) or $TBA^+{\cdot}Br^-$, gave $\mathbf{DH3}_{X2}$ (X = H^+ or TBA^+) or $\mathbf{DH4}_{TBA2}$, respectively (for details, see the Supporting Information).

The X-ray crystallographic analysis of the $\mathbf{DH4}_{H2}$ single crystals grown by slow diffusion of *n*-hexane into a THF solution of $\mathbf{DH4}_{H2}$ in the presence of TFA (3 equiv) revealed that $\mathbf{DH4}_{H2}$ adopts a contracted double-stranded helical structure with a pseudo-D_2-symmetry, the two ligand strands are intertwined with each other bridged by two spiroborate groups, and the two terminal benzene rings of each strand were twisted by ca. 280° (Figure 2a). The structural features of $\mathbf{DH4}_{H2}$ resemble the contracted helical structures of **1** and **2**. All of the *N*-oxide oxygen atoms are positioned at the outside of the double helix, and the terminal ^{t}Bu and phenyl groups are placed on the pyridyl rings of

DOI: 10.1021/jacs.6b00787
J. Am. Chem. Soc. 2016, 138, 4852–4859

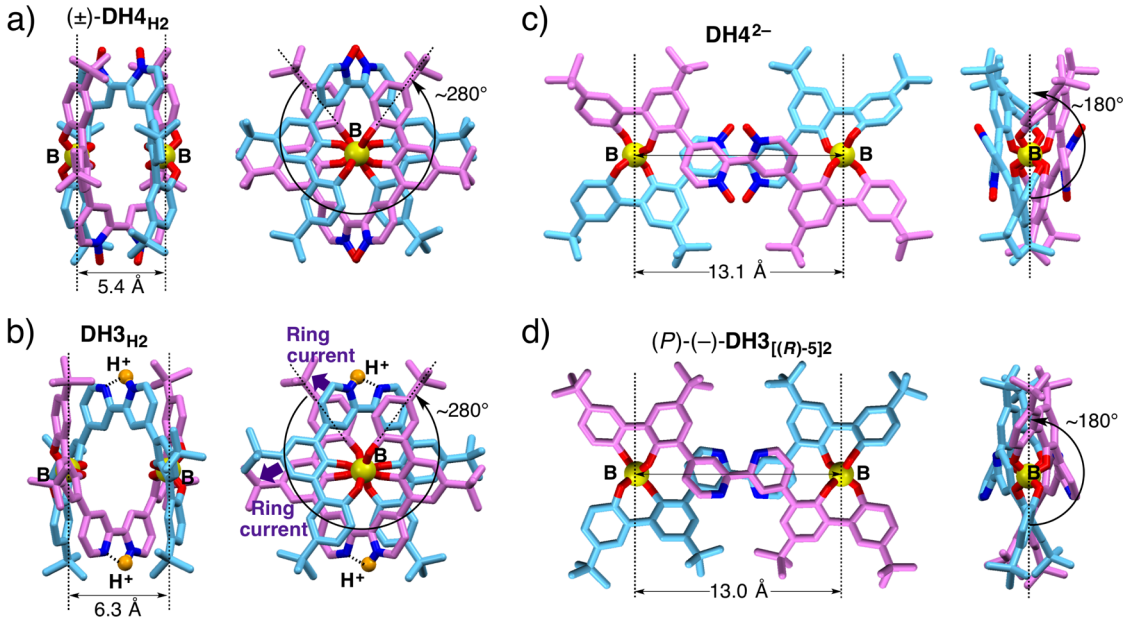

Figure 2. (a,d) X-ray crystal structures of (±)-$\mathbf{DH4}_{\mathbf{H2}}$ (a) and (−)-$\mathbf{DH3}_{[(R)\text{-}5]2}$ (d). All hydrogen atoms are omitted for clarity. For (a), a right-handed double-helical structure is only depicted. (b,c) The energy-minimized right-handed double-helical structures of contracted $\mathbf{DH3}_{\mathbf{H2}}$ (b) and extended $\mathbf{DH4}^{2-}$ (c) obtained by DFT calculations. All hydrogen atoms are omitted for clarity. Protons (H^+) are highlighted as an orange ball.

Scheme 1. Optical Resolution of (±)-$\mathbf{DH3}_{\mathbf{Na2}}$ and (±)-$\mathbf{DH4}_{\mathbf{H2}}$ by the Formation of Diastereomeric Salts with Chiral Ammonium (*S*)- or (*R*)-$\mathbf{5}^{+}\cdot\mathbf{I}^{-}$ and (*S*)- or (*R*)-$\mathbf{6}^{+}\cdot\mathbf{I}^{-}$, Respectively[a]

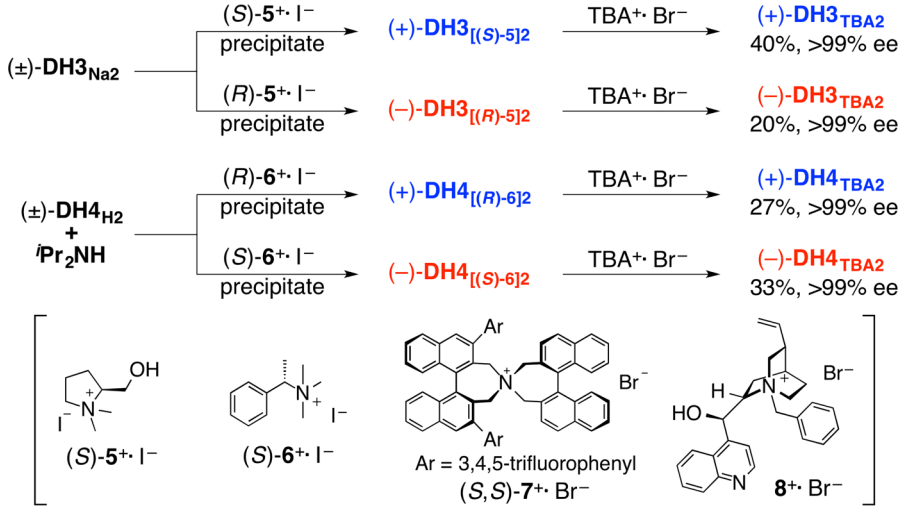

[a]The chiral ammonium **5** and **6** were then replaced with achiral ammonium salt $TBA^{+}\cdot Br^{-}$. The prefixes (+) and (−) denote the signs of the Cotton effect at 336 nm.

the other strand. In contrast to the analogous contracted double helicates of **1** and **2** embedding one or two Na^+ ions in the center,[5,7,8] no Na^+ ion was embraced in the contracted helicate $\mathbf{DH4}_{\mathbf{H2}}$, while maintaining its short B−B distance (5.4 Å), which was significantly shorter than those of the contracted **1a** (6.0 Å)[5a] and **1b** (6.3 Å)[7] and close to that of **2** (5.3 Å).[8] Based on an extremely short distance (2.4 Å) between the negatively charged *N*-oxide oxygen atoms at the same linkers in the crystal, we presumed that each of the two protons is strongly bound to the two *N*-oxide oxygen atoms at each linker moiety through an O···H^+···O hydrogen-bond interaction.[15] This speculation was further supported by the density functional theory (DFT) calculations of $\mathbf{DH4}_{\mathbf{H2}}$ in which such O···H^+···O interactions with the average O−H^+ distance of 1.20 Å were found in the energy-minimized structure with the total charge of zero (Figure S3a).[16] Similarly, the DFT calculations of the protonated $\mathbf{DH3}_{\mathbf{H2}}$ bearing the bpy linkers resulted in the double-helical structure stabilized by the two N^+−H···N interactions at each bpy linker with the *syn* conformation, and its B−B distance was 6.3 Å (Figures 2b and S4a).[17]

The ^{1}H NMR spectra of $\mathbf{DH3}_{\mathbf{H2}}$ in DMSO-d_6[18] and $\mathbf{DH4}_{\mathbf{H2}}$ in CD_3CN displayed one set of signals due to their pseudo-D_2-symmetric structures as were observed in the solid state and/or calculated structures, in which broad signals assigned to the protons bound to the bpy and its *N*,*N*′-dioxide residues were observed at 15.12 and 17.25 ppm for $\mathbf{DH3}_{\mathbf{H2}}$ and $\mathbf{DH4}_{\mathbf{H2}}$, respectively (Figures S6b and S7b). The terminal ^{t}Bu signals and the aromatic protons on the terminal benzene rings were

DOI: 10.1021/jacs.6b00787
J. Am. Chem. Soc. 2016, 138, 4852−4859

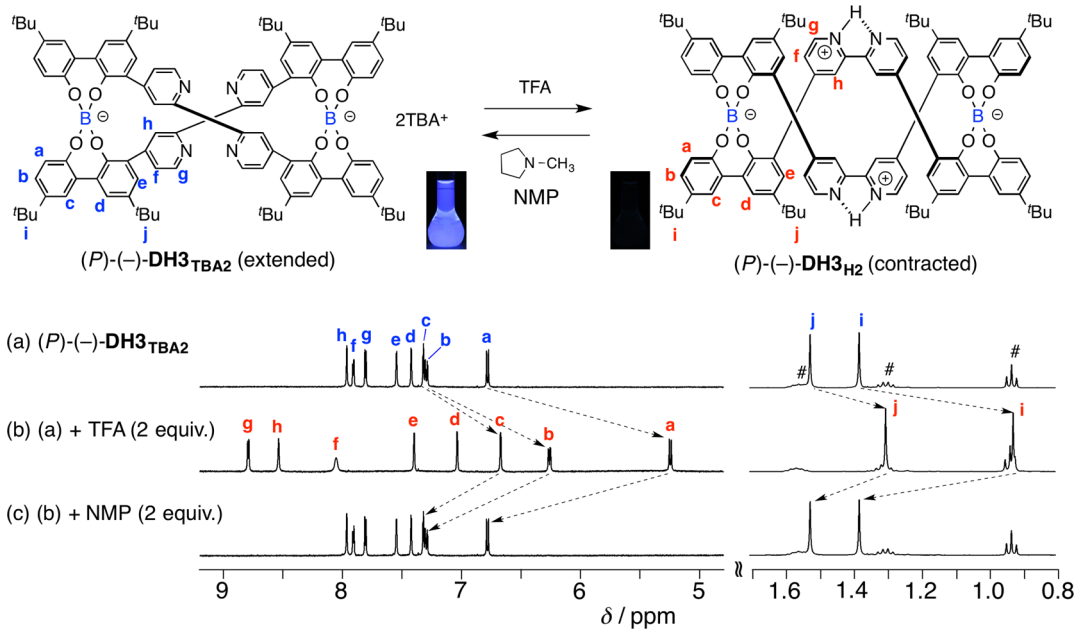

Figure 3. Partial ^{1}H NMR spectra (500 MHz, DMSO-d_6, 0.6 mM, 25 °C) of (*P*)-(−)-**DH3**$_{TBA2}$ (a), (a) + TFA (2 equiv) (b), and (b) + NMP (2 equiv) (c). # denotes the protons from TBA$^+$. Photographs of a DMSO solution of (*P*)-(−)-**DH3**$_{TBA2}$ (10 μM) before and after the addition of TFA (2 equiv) under irradiation at 365 nm are also shown.[23]

significantly shifted upfield as compared to those of the corresponding ligands **L3** and **L4** due to the ring current effect of the pyridyl rings of the other strand (Figures S6a,b and S7a,b; for complete signal assignments, see two-dimensional (2D) COSY and NOESY spectra (Figures S8−S12 for **DH3**$_{H2}$ and Figures S13−S16 for **DH4**$_{H2}$)), which are consistent with their crystal and/or calculated structures (Figures 2a,b, S3a, and S4a). Furthermore, their 2D NOESY spectra showed characteristic interstrand NOE cross-peaks (Figures S11 and S12 for **DH3**$_{H2}$ and Figures S16 for **DH4**$_{H2}$), thus indicating that these helicates retained the contracted double-helical structures in solution.

The racemic helicates (±)-**DH3**$_{Na2}$ and (±)-**DH4**$_{H2}$ were successfully resolved into the enantiomers by diastereomeric salt formation through a cation exchange with (*R*)- or (*S*)-**5**$^+$·I$^-$ and (*S*)- or (*R*)-**6**$^+$·I$^-$, followed by a further cation exchange with the achiral TBA$^+$·Br$^-$ salt, affording the corresponding pairs of the enantiomeric double-stranded helicates ((−)- and (+)-**DH3**$_{TBA2}$ and (−)- and (+)-**DH4**$_{TBA2}$), respectively (Scheme 1). The enantiomeric excess (ee) values of the resolved helicates were determined to be >99% by the ^{1}H NMR measurements in the presence of (*S*,*S*)-**7**$^+$·Br$^-$ (for **DH3**$_{TBA2}$) and *N*-benzylcinchonidinum bromide **8**$^+$·Br$^-$ (for **DH4**$_{TBA2}$) as a chiral shift reagent (Scheme 1 and Figures S26, and S27).[19] Each pair of enantiomers exhibited perfectly mirror-imaged CD spectra (Figures 4a for **DH3**$_{TBA2}$ and 4b for **DH4**$_{TBA2}$).

The single-crystal X-ray analysis of the optically resolved diastereomer (−)-**DH3**$_{[(R)\text{-}5]2}$ allowed us to unambiguously determine its helical sense thanks to the absolute configuration of the countercation (*R*)-**5**$^+$. Interestingly, (−)-**DH3**$_{[(R)\text{-}5]2}$ adopts an extended right-handed (*P*)-double-helical structure with the *anti*-conformation of the bpy linkers, whose B−B distance (13.0 Å) was approximately two times longer than that of the DFT-calculated structure of the contracted **DH3**$_{H2}$ (6.3 Å) with the *syn*-conformation as a result of an unwinding of the contracted helicate through a unidirectional twisting in which the twist angle between the two terminal benzene rings of each strand was changed from ca. 280 to ca. 180° (Figure 2b,d). The CD spectral pattern of the obtained single crystal dissolved in DMSO was almost identical to that of (−)-**DH3**$_{TBA2}$ (Figures 4a and S29). Moreover, the direct *N*-oxidation of the bpy moieties of (*P*)-(−)-**DH3**$_{TBA2}$ by *m*-chloroperoxybenzoic acid resulted in the formation of (*P*)-(−)-**DH4**$_{TBA2}$ with a decrease in the ee value from >99% to ca. 40% due to partial racemization during the reaction (Figure S30; for details, see the Supporting Information). Nevertheless, the resulting CD spectral pattern was nearly identical to that of the enantiopure (−)-**DH4**$_{TBA2}$ obtained by the optical resolution of its racemate (Figure S30c). Therefore, the absolute handedness of both the helical (−)-**DH3**$_{TBA2}$ and (−)-**DH4**$_{TBA2}$ could be determined to be a (*P*)-double-helical structure ((*P*)-(−)-**DH3**$_{TBA2}$ and -**DH4**$_{TBA2}$).

Interestingly, the ^{1}H NMR spectra of **DH3**$_{TBA2}$ in DMSO-d_6 and **DH4**$_{TBA2}$ in CD_3CN were quite different from those of the corresponding protonated helicates **DH3**$_{H2}$ and **DH4**$_{H2}$ (Figures S6b,c and S7b,c; for complete signal assignments, see 2D COSY and NOESY spectra (Figures S17−S21 for **DH3**$_{TBA2}$ and S22−S25 for **DH4**$_{TBA2}$)), respectively. In particular, the terminal ^{t}Bu signals and the aromatic protons on the terminal benzene rings showed significant downfield shifts as compared to those of the corresponding protonated helicates indicating the absence of the ring current effect as discussed above (Figures S6 and S7). This observation in addition to the absence of interstrand cross-peaks in the NOESY spectra of **DH3**$_{TBA2}$ and **DH4**$_{TBA2}$ (Figures S19−S21 and S24−S25) indicated that these helicates retained the extended double-helical structures in solution similar to those of (−)-**DH3**$_{[(R)\text{-}5]2}$ in the solid state and **DH4**$^{2-}$ obtained by the DFT calculations (Figure 2).

Although the contracted helicate **1a** is stabilized by coordination of the embedded Na$^+$ ion to the oxygen atoms of the spiroborate moieties in CH_3CN,[5a] **DH3**$_{Na2}$ having two Na$^+$ ions adopted the extended form in DMSO-d_6 as indicated by its ^{1}H NMR spectrum being identical to that of **DH3**$_{TBA2}$ (Figure S6c,d). This is because the Na$^+$ ions are highly solvated with polar DMSO molecules that prevent the Na$^+$ ion being entrapped within the helicate cavity of **DH3**$_{Na2}$, leading to release of the Na$^+$

DOI: 10.1021/jacs.6b00787
J. Am. Chem. Soc. 2016, 138, 4852−4859

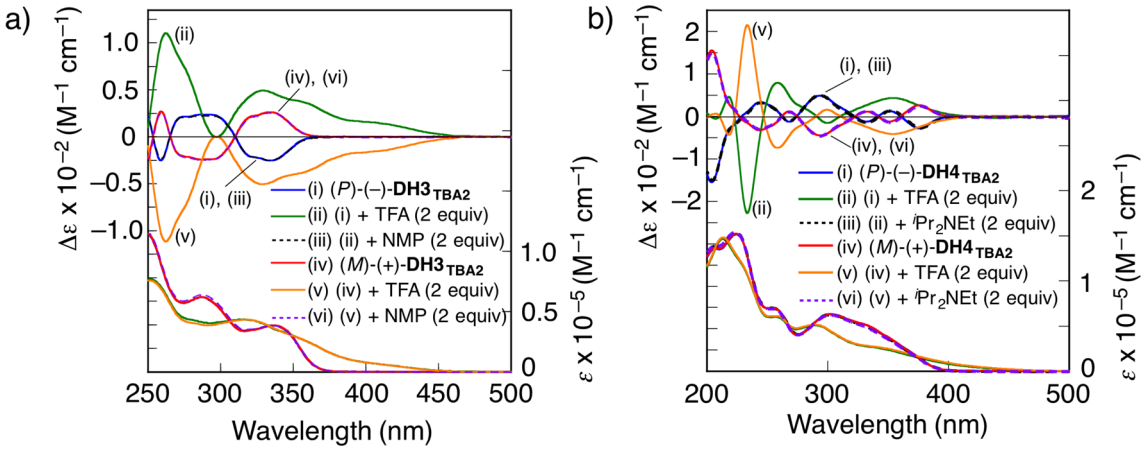

Figure 4. (a) CD and absorption spectra (DMSO-d_6, 0.6 mM, ca. 25 °C) of (*P*)-(−)-**DH3**$_{TBA2}$ (i), (i) + TFA (2 equiv) (ii), (ii) + NMP (2 equiv) (iii), (*M*)-(+)-**DH3**$_{TBA2}$ (iv), (iv) + TFA (2 equiv) (v), and (v) + NMP (2 equiv) (vi). (b) CD and absorption spectra (CD_3CN, 0.6 mM, ca. 25 °C) of (*P*)-(−)-**DH4**$_{TBA2}$ (i), (i) + TFA (2 equiv) (ii), (ii) + $^iPr_2NEt$ (2 equiv) (iii), (*M*)-(+)-**DH4**$_{TBA2}$ (iv), (iv) + TFA (2 equiv) (v), and (v) + $^iPr_2NEt$ (2 equiv) (vi).

ion in DMSO. In contrast, upon the addition of $NaPF_6$ to a solution of the extended helicate **DH3**$_{TBA2}$ in CD_3CN, a new set of signals corresponding to the contracted helicate appeared in its ^1H NMR spectrum (Figure S31), although the resulting contracted **DH3**$_{Na2}$ was partially precipitated due to its low solubility in CD_3CN. However, the binding constant (K_b) of **DH3**$_{TBA2}$ to the Na^+ ion was much lower than that of **1a** (K_b = 2.68 × 10^6 M^{-1}),[5a] as supported by the competitive binding experiment using an equimolar mixture of **DH3**$_{TBA2}$ and **1a**$_{Na\cdot BMA}$[5a] (BMA = benzyltrimethylammonium) in CD_3CN by ^1H NMR spectroscopy, showing no trace amount of the **DH3**$_{Na\cdot X}$ species (X = TBA, Na, or BMA) (Figure S32). A similar weak binding affinity of the extended helicate **DH4**$_{TBA2}$ to the Na^+ ion was also confirmed in CD_3CN,[20] indicating that contracted forms of the **DH3**$_{Na\cdot X}$ and **DH4**$_{Na\cdot X}$ (X = TBA) helicates embracing a Na^+ ion in the center are unstable, most likely due to a thermodynamically unfavorable *syn*-conformation of the bpy and its *N*,*N*′-dioxide moieties. These results suggest that the helicates **DH3** and **DH4** may not be suitable as a Na^+ ion-triggered molecular spring.

However, taking advantage of the *syn*-conformation preference of bpy[11] and its *N*,*N*′-dioxide groups[21] in the presence of protons and metals, the fully reversible extension−contraction motions of the helicates accompanied by unidirectional twisting were found to proceed in a highly cooperative, allosteric fashion by external stimuli, such as the combination of an acid and base or Cu^{2+} and tren (tren = tris(2-aminoethyl)amine) when enantiopure helicates were used.

The addition of 2 equiv of TFA to a solution of the (*P*)-(−)- or (*M*)-(+)-enantiomer of the extended **DH3**$_{TBA2}$ in DMSO-d_6 resulted in full conversion to the contracted helicate as confirmed by its ^1H NMR spectrum which is identical to that of the contracted **DH3**$_{H2}$ (Figures 3a,b and S6b).[22] This conformational transition led to the remarkable CD spectral changes with an inversion of the first Cotton effect sign accompanied by the appearance of a shoulder absorption band around 350−450 nm (Figure 4a). These NMR, CD, and absorption spectra were completely switched back to the original ones by the subsequent addition of 2 equiv of *N*-methylpyrrolidine (NMP) as a base resulting from the quantitative extended helicate formation (Figures 3 and 4a).[23] Importantly, the CD spectra of (*P*)-(−)- and (*M*)-(+)-**DH3**$_{TBA2}$ remained unchanged during the dynamic extension−contraction motions (Figure 4a), thus indicating that no racemization took place during the acid/base-triggered reversible extension−contraction motions coupled with twisting in one direction.

A similar helical structural change can also be controlled by the sequential addition of $Cu(NO_3)_2{\cdot}3H_2O$ (2 equiv) and tren (2 equiv) to the extended (*P*)-(−)-**DH3**$_{TBA2}$ that readily and reversibly underwent a unidirectional spring-like motion while maintaining its one-handed helical chirality in which the Cu^{2+} ions coordinated to each bpy unit induce the *syn* conformational change, thus triggering the contraction motion, which further quantitatively reverted back to the original extracted helicate by tren being a stronger chelating agent (Figure S35). The right-handed helicate (*P*)-(−)-**DH4**$_{TBA2}$ also showed a reversible extension−contraction motion upon the alternative addition of TFA and *N*,*N*-diisopropylethylamine ($^iPr_2NEt$) in CD_3CN, resulting in the complete reversible ^1H NMR, CD, and absorption spectral changes (Figures 4b and S36).

To gain further insight into the proton binding behavior of the extended helicates leading to a spring-like motion, the ^1H NMR titration experiments of TFA with **DH3**$_{TBA2}$ in DMSO-d_6 and with **DH4**$_{TBA2}$ in CD_3CN were carried out. Interestingly, only two sets of signals corresponding to the nonprotonated (extended) and diprotonated (contracted) helicates were observed for both systems in the presence of less than 2 equiv of TFA, in which the mole fractions of the diprotonated helicates **DH3**$_{H2}$ and **DH4**$_{H2}$ linearly increased with an increase in the amount of TFA,[24] indicating a slow exchange between the extended and contracted forms on the present NMR time scale (Figures S37 and S38). Despite the slow exchange, however, a monoprotonated helicate, such as **DH3**$_{H\cdot TBA}$ and **DH4**$_{H\cdot TBA}$, could not be observed at all upon the addition of TFA (Figures S37 and S38), demonstrating a strong positive cooperativity, namely, the first proton binding to one of the two binding sites (bpy or its *N*,*N*′-dioxide units) enforces the orientation of the other site in such a way that the second proton binding is significantly facilitated.

In order to quantitatively estimate the cooperativity according to the Hill equation,[25] the UV−vis titration of TFA with **DH4**$_{TBA2}$ was performed. The absorption spectral changes of a highly diluted DMSO solution of **DH4**$_{TBA2}$ (10 μM) upon the addition of TFA showed clear isosbestic points at 384 and 294

DOI: 10.1021/jacs.6b00787
J. Am. Chem. Soc. 2016, 138, 4852−4859

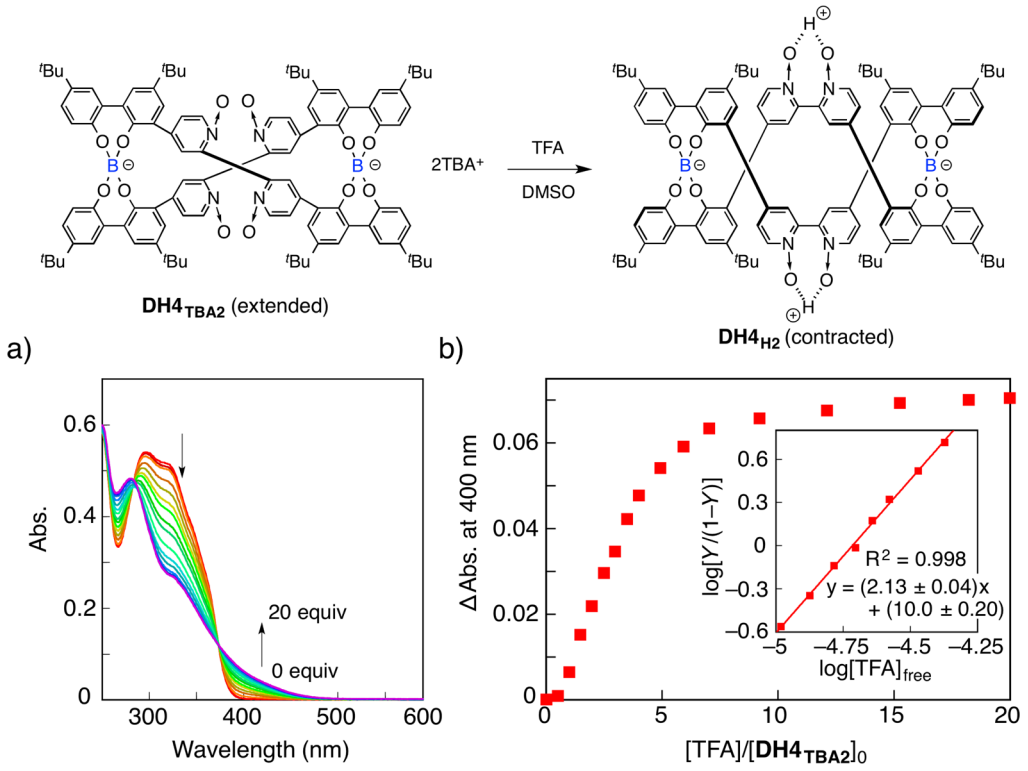

Figure 5. (a) UV−vis titrations of $\mathbf{DH4}_{\mathbf{TBA2}}$ (10 mM) with TFA in DMSO at 25 °C. (b) Plots of absorption intensity changes (ΔAbs) at 400 nm for $\mathbf{DH4}_{\mathbf{TBA2}}$ as a function of $[\mathrm{TFA}]/[\mathbf{DH4}_{\mathbf{TBA2}}]_0$. Inset shows the Hill plot for the binding of TFA to $\mathbf{DH4}_{\mathbf{TBA2}}$. $Y = \Delta\mathrm{Abs}/\Delta\mathrm{Abs}_{max}$.

nm. The plots of the absorbance at 400 nm versus the TFA concentration displayed a sigmoidal curvature characteristic of the positive homotropic allosterism (Figure 5).[26] The Hill coefficient (n_H = 2.1 ± 0.04) and the apparent association constant (log K_a = 10.0 ± 0.20 (M^{-2})) were obtained from the Hill plot[25] (Figure 5b; for details, see the Supporting Information). The n_H value is almost equal to the maximum value identical to the number of binding sites, being reasonably consistent with the previous ^{1}H NMR results that showed no signal due to the monoprotonated helicate (Figure S38). In the same way, we attempted to estimate the n_H and K_a values for $\mathbf{DH3}_{\mathbf{TBA2}}$, but it was difficult because the K_a value was too high to accurately estimate, which is at least approximately 10^5 times higher than that of $\mathbf{DH4}_{\mathbf{TBA2}}$ based on the competitive binding experiment using $\mathbf{DH3}_{\mathbf{H2}}$ in the presence of 10 equiv of $\mathbf{DH4}_{\mathbf{TBA2}}$ in DMSO-d_6 by ^{1}H NMR spectroscopy, giving no new signals derived from $\mathbf{DH3}_{\mathbf{TBA2}}$ and $\mathbf{DH4}_{\mathbf{H2}}$ (Figure S39). Surprisingly, the apparent K_a values of the ligands **L3** (K_a = ca. 7.1 × 10^2 M^{-1}) and **L4** (K_a = ca. 1.2 × 10^2 M^{-1}) with protons were much lower than those of the corresponding helicates (Figures S40 and S41), clearly indicating a strong positive cooperativity; the anionic nature of the helicates may more or less contribute to this high cooperativity.

Finally, the kinetics of the proton-assisted extension and contraction events of the helicates (**DH3** and **DH4**) was investigated by the 2D EXSY measurements[27] of a 1:1 mixture of the extended and contracted helicates generated with 1 equiv of TFA in DMSO-d_6 at 25 °C, which showed a number of chemical exchange cross-peaks between the extended/contracted helicates ($\mathbf{DH3}_{\mathbf{TBA2}}/\mathbf{DH3}_{\mathbf{H2}}$ and $\mathbf{DH4}_{\mathbf{TBA2}}/\mathbf{DH4}_{\mathbf{H2}}$) (Figures S42 and S43). By measuring the peak volumes of the cross and diagonal peaks at different mixing times, the apparent exchange rate constants (k_{ex}) between the extended/contracted helicates ($(\mathbf{DH3}_{\mathbf{TBA2}}/\mathbf{DH3}_{\mathbf{H2}}$ and $\mathbf{DH4}_{\mathbf{TBA2}}/\mathbf{DH4}_{\mathbf{H2}})$) were estimated to be 5.18 and 38.5 s^{-1}, respectively. These results indicated that the proton-assisted extension and contraction motion of **DH3** bearing bpy units is approximately 7 times slower than that of **DH4** bearing *N*,*N*′-dioxide-bpy units (Figures S42 and S43; for details, see the Supporting Information). The slower elastic rate observed for **DH3** could be ascribed to its higher binding affinity than **DH4** toward protons.

CONCLUSIONS

In summary, we have found unique allosterically regulated reversible extension and contraction motions coupled with unidirectional twisting in enantiomeric double-stranded spiroborate helicates bearing the 2,2′-bpy and its *N*,*N*′-dioxide linkages in the middle of the strands, while maintaining their helical handedness. X-ray crystallography together with DFT calculations and 2D NMR and CD spectroscopies unraveled the mechanistic details and kinetics of the allosteric spring-like motions; the cooperative binding and release of protons and/or Cu^{2+} ions to the two covalently linked bpy or its *N*,*N*′-dioxide linkages spontaneously induce local conformational changes, i.e., *anti*-to-*syn* and *syn*-to-*anti* isomerization at the binding sites of the linkages, respectively. Most importantly, these small conformational changes that occurred at the linkages are further significantly amplified to a large-scale conformational transition of the overall helical structures of the helicates[28] leading to unidirectional elastic motions in a highly positive, homotropic allosteric manner. These findings may provide a rational design strategy for developing a conceptually new, allosterically regulated supramolecular asymmetric catalyst[2f,g,29] whose catalytic activity and enantioselectivity will be modulated by a unidirectional elastic motion,[30] since the catalytically active bpy-

DOI: 10.1021/jacs.6b00787
J. Am. Chem. Soc. 2016, 138, 4852−4859

N,*N*′-dioxide residues are twisted in one direction by a different twist angle during the chiral elastic motion.

■ ASSOCIATED CONTENT

Supporting Information

The Supporting Information is available free of charge on the ACS Publications website at DOI: 10.1021/jacs.6b00787.

Experimental procedures, characterizations of ligands **L3** and **L4** and helicates $\mathbf{DH3}_{X2}$ (X = Na^+, H^+, or TBA^+) and $\mathbf{DH4}_{X2}$ (X = H^+ or TBA^+), and additional spectroscopic data. (PDF)

X-ray crystallographic data for $\mathbf{DH3}_{[(R)\text{-}5]2}$ (CIF; CCDC 1445714) (CIF)

X-ray crystallographic data for $\mathbf{DH4}_{H2}$ (CIF; CCDC 1445715) (CIF)

■ AUTHOR INFORMATION

Corresponding Author

*yashima@apchem.nagoya-u.ac.jp

Present Address

†Department of Chemistry, Interdisciplinary Graduate School of Science and Engineering, Shimane University, 1060 Nishikawatsu, Matsue 690−8504, Japan.

Notes

The authors declare no competing financial interest.

■ ACKNOWLEDGMENTS

This work was supported in part by JSPS KAKENHI (Grant-in-Aid for Scientific Research (S), no. 25220804 (E.Y.) and Grant-in-Aid for Young Scientists (B), no. 26810047 (N.O.)) The authors thank Kaori Shimizu and Dr. Daisuke Taura for their help in the synthesis of $\mathbf{DH3}_{Na2}$ and $\mathbf{DH4}_{H2}$ and Shinya Yamamoto for his help with the single crystal X-ray diffraction measurements.

■ REFERENCES

(1) (a) Monod, J.; Wyman, J.; Changeux, J.-P. *J. Mol. Biol.* **1965**, *12*, 88−118. (b) Cantor, R. C.; Schimmel, P. R. *Biophysical Chemistry*, Part III; Freeman: New York, 1980. (c) Berg, J. M.; Stryer, L.; Tymoczko, J. L. *Biochemistry*, 5th ed.; Freeman: New York, 2002.

(2) For reviews of syntheic allosteric receptors and catalysts, see: (a) Rebek, J., Jr. *Acc. Chem. Res.* **1984**, *17*, 258−264. (b) Nabeshima, T. *Coord. Chem. Rev.* **1996**, *148*, 151−169. (c) Shinkai, S.; Ikeda, M.; Sugasaki, A.; Takeuchi, M. *Acc. Chem. Res.* **2001**, *34*, 494−503. (d) Takeuchi, M.; Ikeda, M.; Sugasaki, A.; Shinkai, S. *Acc. Chem. Res.* **2001**, *34*, 865−873. (e) Kovbasyuk, L.; Krämer, R. *Chem. Rev.* **2004**, *104*, 3161−3188. (f) Oliveri, C. G.; Ulmann, P. A.; Wiester, M. J.; Mirkin, C. A. *Acc. Chem. Res.* **2008**, *41*, 1618−1629. (g) Wiester, M. J.; Ulmann, P. A.; Mirkin, C. A. *Angew. Chem., Int. Ed.* **2011**, *50*, 114−137. (h) McConnell, A. J.; Beer, P. D. *Angew. Chem., Int. Ed.* **2012**, *51*, 5052−5061. (i) Kremer, C.; Lützen, A. *Chem. - Eur. J.* **2013**, *19*, 6162−6196.

(3) For reviews of artificial molecular machines, see: (a) Urry, D. W. *Angew. Chem., Int. Ed. Engl.* **1993**, *32*, 819−841. (b) Balzani, V.; Credi, A.; Raymo, F. M.; Stoddart, J. F. *Angew. Chem., Int. Ed.* **2000**, *39*, 3349−3391. (c) Ballardini, R.; Balzani, V.; Credi, A.; Gandolfi, M. T.; Venturi, M. *Acc. Chem. Res.* **2001**, *34*, 445−455. (d) Collin, J. P.; Dietrich-Buchecker, C.; Gaviña, P.; Jimenez-Molero, M. C.; Sauvage, J. P. *Acc. Chem. Res.* **2001**, *34*, 477−487. (e) Kelly, T. R. *Acc. Chem. Res.* **2001**, *34*, 514−522. (f) Schalley, C. A.; Beizai, K.; Vogtle, F. *Acc. Chem. Res.* **2001**, *34*, 465−476. (g) Kinbara, K.; Aida, T. *Chem. Rev.* **2005**, *105*, 1377−1400. (h) Kottas, G. S.; Clarke, L. I.; Horinek, D.; Michl, J. *Chem. Rev.* **2005**, *105*, 1281−1376. (i) Feringa, B. L. *J. Org. Chem.* **2007**, *72*, 6635−6652. (j) Saha, S.; Stoddart, J. F. *Chem. Soc. Rev.* **2007**, *36*, 77−92. (k) Coskun, A.; Banaszak, M.; Astumian, R. D.; Stoddart, J. F.; Grzybowski, B. A. *Chem. Soc. Rev.* **2012**, *41*, 19−30. (l) Bruns, C. J.; Stoddart, J. F. *Acc. Chem. Res.* **2014**, *47*, 2186−2199. (m) Erbas-Cakmak, S.; Leigh, D. A.; McTernan, C. T.; Nussbaumer, A. L. *Chem. Rev.* **2015**, *115*, 10081−10206.

(4) For examples of a spring-like motion of helical oligomers and polymers triggered by external stimuli, see: (a) Jung, O.-S.; Kim, Y. J.; Lee, Y.-A.; Park, J. K.; Chae, H. K. *J. Am. Chem. Soc.* **2000**, *122*, 9921−9925. (b) Yashima, E.; Maeda, K.; Sato, O. *J. Am. Chem. Soc.* **2001**, *123*, 8159−8160. (c) Barboiu, M.; Vaughan, G.; Kyritsakas, N.; Lehn, J. M. *Chem. - Eur. J.* **2003**, *9*, 763−769. (d) Nabeshima, T.; Yoshihira, Y.; Saiki, T.; Akine, S.; Horn, E. *J. Am. Chem. Soc.* **2003**, *125*, 28−29. (e) Pengo, P.; Pasquato, L.; Moro, S.; Brigo, A.; Fogolari, F.; Broxterman, Q. B.; Kaptein, B.; Scrimin, P. *Angew. Chem., Int. Ed.* **2003**, *42*, 3388−3392. (f) Zhao, H.; Sanda, F.; Masuda, T. *J. Polym. Sci., Part A: Polym. Chem.* **2005**, *43*, 5168−5176. (g) Maeda, K.; Mochizuki, H.; Watanabe, M.; Yashima, E. *J. Am. Chem. Soc.* **2006**, *128*, 7639−7650. (h) Berni, E.; Kauffmann, B.; Bao, C. Y.; Lefeuvre, J.; Bassani, D. M.; Huc, I. *Chem. - Eur. J.* **2007**, *13*, 8463−8469. (i) Kim, H.-J.; Lee, E.; Park, H.-s.; Lee, M. *J. Am. Chem. Soc.* **2007**, *129*, 10994−10995. (j) Kakuchi, R.; Nagata, S.; Sakai, R.; Otsuka, I.; Nakade, H.; Satoh, T.; Kakuchi, T. *Chem. - Eur. J.* **2008**, *14*, 10259−10266. (k) Percec, V.; Rudick, J. G.; Peterca, M.; Heiney, P. A. *J. Am. Chem. Soc.* **2008**, *130*, 7503−7508. (l) Ferrand, Y.; Kendhale, A. M.; Garric, J.; Kauffmann, B.; Huc, I. *Angew. Chem., Int. Ed.* **2010**, *49*, 1778−1781. (m) Hashimoto, T.; Nishimura, T.; Lim, J. M.; Kim, D.; Maeda, H. *Chem. - Eur. J.* **2010**, *16*, 11653−11661. (n) Ferrand, Y.; Gan, Q.; Kauffmann, B.; Jiang, H.; Huc, I. *Angew. Chem., Int. Ed.* **2011**, *50*, 7572−7575. (o) Ohta, E.; Sato, H.; Ando, S.; Kosaka, A.; Fukushima, T.; Hashizume, D.; Yamasaki, M.; Hasegawa, K.; Muraoka, A.; Ushiyama, H.; Yamashita, K.; Aida, T. *Nat. Chem.* **2011**, *3*, 68−73. (p) Leiras, S.; Freire, F.; Seco, J. M.; Quiñoá, E.; Riguera, R. *Chem. Sci.* **2013**, *4*, 2735−2743. (q) Maeda, H.; Nishimura, T.; Akuta, R.; Takaishi, K.; Uchiyama, M.; Muranaka, A. *Chem. Sci.* **2013**, *4*, 1204−1211. (r) Yoshida, Y.; Mawatari, Y.; Motoshige, A.; Motoshige, R.; Hiraoki, T.; Wagner, M.; Müllen, K.; Tabata, M. *J. Am. Chem. Soc.* **2013**, *135*, 4110−4116.

(5) (a) Miwa, K.; Furusho, Y.; Yashima, E. *Nat. Chem.* **2010**, *2*, 444−449. (b) Miwa, K.; Shimizu, K.; Min, H.; Furusho, Y.; Yashima, E. *Tetrahedron* **2012**, *68*, 4470−4478.

(6) An analogous helicate bearing photoresponsive stilleben linkers also showed a similar spring-like motion; see: Taura, D.; Min, H.; Katan, C.; Yashima, E. *New J. Chem.* **2015**, *39*, 3259−3269.

(7) Katagiri, H.; Miyagawa, T.; Furusho, Y.; Yashima, E. *Angew. Chem., Int. Ed.* **2006**, *45*, 1741−1744.

(8) Furusho, Y.; Miwa, K.; Asai, R.; Yashima, E. *Chem. - Eur. J.* **2011**, *17*, 13954−13957.

(9) A double-stranded porphyrin-linked spiroborate helicate underwent unidirectional dual rotary and twisting motions through inclusion of an aromatic guest molecule; see: Yamamoto, S.; Iida, H.; Yashima, E. *Angew. Chem., Int. Ed.* **2013**, *52*, 6849−6853.

(10) Optically active 2,2′-bpy *N*,*N*′-dioxide derivatives are known to catalyze asymmetric reactions. For examples, see: (a) Shimada, T.; Kina, A.; Ikeda, S.; Hayashi, T. *Org. Lett.* **2002**, *4*, 2799−2801. (b) Shimada, T.; Kina, A.; Hayashi, T. *J. Org. Chem.* **2003**, *68*, 6329−6337.

(11) The monoprotonated 2,2′-bpy has been reported to preferentially adopt a *syn* conformer rather than a less sterically hindered *anti* one due to an N^+−H···N interaction. For examples, see: (a) Howard, S. T. *J. Am. Chem. Soc.* **1996**, *118*, 10269−10274. (b) Zahn, S.; Reckien, W.; Kirchner, B.; Staats, H.; Matthey, J.; Lützen, A. *Chem. - Eur. J.* **2009**, *15*, 2572−2580.

(12) (a) Chalmers, R.; Guhathakurta, A.; Benjamin, H.; Kleckner, N. *Cell* **1998**, *93*, 897−908. (b) He, X. L.; Chow, D. C.; Martick, M. M.; Garcia, K. C. *Science* **2001**, *293*, 1657−1662. (c) Schoenauer, R.; Bertoncini, P.; Machaidze, G.; Aebi, U.; Perriard, J. C.; Hegner, M.; Agarkova, I. *J. Mol. Biol.* **2005**, *349*, 367−379. (d) Nishinaka, T.; Doi, Y.; Hara, R.; Yashima, E. *J. Mol. Biol.* **2007**, *370*, 837−845.

(13) A treatment of **L4** with $NaBH_4$ resulted in a mixture of unknown products.

(14) The countercation species of as-prepared $\mathbf{DH4}_{H2}$ was assigned to the protons rather than Na^+ ions, as supported by a monovalent anion

DOI: 10.1021/jacs.6b00787
J. Am. Chem. Soc. 2016, 138, 4852−4859

[$\mathbf{DH4_{H2}} - H^+$]$^-$ peak in its electrospray ionization (ESI) mass spectrum (Figure S5d), so that countercation exchange with TBA$^+$·Br$^-$ was carried out in the presence of 3 equiv of diisopropylamine (^{i}Pr$_2$NH) to extract the protons from $\mathbf{DH4_{H2}}$.

(15) A similar O···H$^+$···O hydrogen-bond interaction was also observed for [(DMSO)$_2$H]$_2$[PtCl$_6$]; see: Denisov, G. S.; Koll, A.; Lobadyuk, V. I.; Schreiber, V. M.; Shurukhina, A. V.; Spevak, V. N. *J. Mol. Struct.* **2002**, *605*, 221−226.

(16) The B−B distance of $\mathbf{DH4_{H2}}$ optimized by the DFT calculations was 5.8 Å, which was slightly longer than that in the crystal state (5.4 Å), probably due to the absence of crystal packing.

(17) Single crystals of $\mathbf{DH3_{H2}}$ suitable for an X-ray analysis could not be obtained, despite various attempts.

(18) $\mathbf{DH3_{H2}}$ is hardly soluble in CH_3CN.

(19) It is noteworthy that the optical resolution of (±)-$\mathbf{DH4_{H2}}$ can be possible by chiral HPLC (Figure S28).

(20) The signals in the ^{1}H NMR spectrum of $\mathbf{DH4_{TBA2}}$ in CD_3CN significantly broadened and only slightly shifted upon the addition of $NaPF_6$ (10 equiv) (Figure S33), indicating very weak binding affinity of the extended helicate $\mathbf{DH4_{TBA2}}$ to the Na^+ ion.

(21) For examples, see: (a) Kanno, H.; Yano, T.; Sato, K.; Utsuno, S.; Fujita, J. *Bull. Chem. Soc. Jpn.* **1997**, *70*, 1085−1091. (b) Kanno, H.; Yamada, M.; Nakata, K.; Nishimura, M. *Inorg. Chim. Acta* **2001**, *318*, 181−185.

(22) The DFT calculations revealed that the contracted helicates $\mathbf{DH3_{H2}}$ and $\mathbf{DH4_{H2}}$ are 18.9 and 40.1 kcal mol^{-1} more stable than the corresponding extended helicates, respectively (Figures S3 and S4), which is in agreement with the experimentally observed, proton-triggered extended helicate formations.

(23) The acid−base triggered spring-like motion of (*P*)-(−)-$\mathbf{DH3_{TBA2}}$ was accompanied by a fluorescence switching (on and off); the fluorescence of (*P*)-(−)-$\mathbf{DH3_{TBA2}}$ was completely quenched by the addition of 2 equiv of TFA, and was then completely recovered by the further addition of 2 equiv of NMP (Figure S34).

(24) The proton signals due to the extended form completely disappeared upon the addition of 2 equiv of TFA, and the further addition of TFA (up to 3 equiv) resulted in almost no change in the NMR spectra (Figures S37 and S38).

(25) Connors, K. A. *Binding Constants*; John Wiley & Sons: New York, 1987.

(26) For examples of supramolecular receptors exhibiting a positive homotropic allosterism, see: (a) Rebek, J., Jr.; Costello, T.; Marshall, L.; Wattley, R.; Gadwood, R. C.; Onan, K. *J. Am. Chem. Soc.* **1985**, *107*, 7481−7487. (b) Takeuchi, M.; Imada, T.; Shinkai, S. *Angew. Chem., Int. Ed.* **1998**, *37*, 2096−2099. (c) Sugasaki, A.; Ikeda, M.; Takeuchi, M.; Shinkai, S. *Angew. Chem., Int. Ed.* **2000**, *39*, 3839−3842. (d) Borovkov, V. V.; Lintuluoto, J. M.; Sugeta, H.; Fujiki, M.; Arakawa, R.; Inoue, Y. *J. Am. Chem. Soc.* **2002**, *124*, 2993−3006. (e) Raker, J.; Glass, T. E. *J. Org. Chem.* **2002**, *67*, 6113−6116. (f) Sessler, J. L.; Maeda, H.; Mizuno, T.; Lynch, V. M.; Furuta, H. *J. Am. Chem. Soc.* **2002**, *124*, 13474−13479. (g) Chang, S. Y.; Um, M. C.; Uh, H.; Jang, H. Y.; Jeong, K. S. *Chem. Commun.* **2003**, 2026−2027. (h) Huang, F. H.; Fronczek, F. R.; Gibson, H. W. *J. Am. Chem. Soc.* **2003**, *125*, 9272−9273. (i) Jones, P. D.; Glass, T. E. *Tetrahedron* **2004**, *60*, 11057−11065. (j) Kawai, H.; Katoono, R.; Nishimura, K.; Matsuda, S.; Fujiwara, K.; Tsuji, T.; Suzuki, T. *J. Am. Chem. Soc.* **2004**, *126*, 5034−5035. (k) Huang, W. H.; Liu, S. M.; Zavalij, P. Y.; Isaacs, L. *J. Am. Chem. Soc.* **2006**, *128*, 14744−14745. (l) Ikeda, T.; Hirata, O.; Takeuchi, M.; Shinkai, S. *J. Am. Chem. Soc.* **2006**, *128*, 16008−16009. (m) Sessler, J. L.; Tomat, E.; Lynch, V. M. *J. Am. Chem. Soc.* **2006**, *128*, 4184−4185. (n) Setsune, J. I.; Watanabe, K. *J. Am. Chem. Soc.* **2008**, *130*, 2404−2405. (o) Willans, C. E.; Anderson, K. M.; Potts, L. C.; Steed, J. W. *Org. Biomol. Chem.* **2009**, *7*, 2756−2760. (p) Park, J. S.; Le Derf, F.; Bejger, C. M.; Lynch, V. M.; Sessler, J. L.; Nielsen, K. A.; Johnsen, C.; Jeppesen, J. O. *Chem. - Eur. J.* **2010**, *16*, 848−854. (q) He, X.; Xu, X. B.; Wang, X.; Zhao, L. *Chem. Commun.* **2013**, *49*, 7153−7155. (r) Bardelang, D.; Casano, G.; Poulhes, F.; Karoui, H.; Filippini, J.; Rockenbauer, A.; Rosas, R.; Monnier, V.; Siri, D.; Gaudel-Siri, A.; Ouari, O.; Tordo, P. *J. Am. Chem. Soc.* **2014**, *136*, 17570−17577. (s) Kumar, M.; George, S. J. *Chem. Sci.* **2014**, *5*, 3025−3030. (t) Saha, I.; Lee, J. H.; Hwang, H.; Kim, T. S.; Lee, C. H. *Chem. Commun.* **2015**, *51*, 5679−5682.

(27) Perrin, C. L.; Dwyer, T. J. *Chem. Rev.* **1990**, *90*, 935−967.

(28) For examples of amplification of molecular motion mediated by *anti-syn* isomerization of the 2,2′-bpy units in chiral macrocycles, see: (a) Haberhauer, G. *Angew. Chem., Int. Ed.* **2008**, *47*, 3635−3638. (b) Haberhauer, G. *Angew. Chem., Int. Ed.* **2010**, *49*, 9286−9289.

(29) (a) Raynal, M.; Ballester, P.; Vidal-Ferran, A.; van Leeuwen, P. W. N. M. *Chem. Soc. Rev.* **2014**, *43*, 1660−1733. (b) Raynal, M.; Ballester, P.; Vidal-Ferran, A.; van Leeuwen, P. W. N. M. *Chem. Soc. Rev.* **2014**, *43*, 1734−1787.

(30) For asymmetric supramolecular catalysts whose enantioselectivity can be tuned by the motion of a molecular motor, see: (a) Wang, J.; Feringa, B. L. *Science* **2011**, *331*, 1429−1432. (b) Vlatković, M.; Bernardi, L.; Otten, E.; Feringa, B. L. *Chem. Commun.* **2014**, *50*, 7773−7775. (c) Zhao, D.; Neubauer, T. M.; Feringa, B. L. *Nat. Commun.* **2015**, *6*, 6652.

DOI: 10.1021/jacs.6b00787
J. Am. Chem. Soc. 2016, 138, 4852−4859